

Novel product specificity toward erlose and panose exhibited by multisite engineered mutants of amylosucrase

Alizée Vergès, Emmanuelle Cambon, Sophie Barbe, Claire Moulis, Magali Remaud-Siméon,* and Isabelle André*

Laboratoire d'Ingénierie des Systèmes Biologiques et des Procédés, Université de Toulouse, CNRS, INRA, INSA, Toulouse, 31400, France

Received 18 October 2016; Accepted 19 December 2016

DOI: 10.1002/pro.3106

Published online 26 December 2016 proteinscience.org

Abstract: A computer-aided engineering approach recently enabled to deeply reshape the active site of *N. polysaccharea* amylosucrase for recognition of non-natural acceptor substrates. Libraries of variants were constructed and screened on sucrose allowing the identification of 17 mutants able to synthesize molecules from sole sucrose, which are not synthesized by the parental wild-type enzyme. Three of the isolated mutants as well as the new products synthesized were characterized in details. Mutants contain between 7 and 11 mutations in the active site and the new molecules were identified as being a sucrose derivative, named erlose (α -D-glucopyranosyl-(1 \rightarrow 4)- α -D-glucopyranosyl-(1 \rightarrow 2)- β -D-Fructose), and a new malto-oligosaccharide named panose (α -D-glucopyranosyl-(1 \rightarrow 6)- α -D-glucopyranosyl-(1 \rightarrow 4)- α -D-Glucose). These product specificities were never reported for none of the amylosucrases characterized to date, nor their engineered variants. Optimization of the production of these trisaccharides of potential interest as sweeteners or prebiotic molecules was carried out. Molecular modelling studies were also performed to shed some light on the molecular factors involved in the novel product specificities of these amylosucrase variants.

Keywords: enzyme engineering; amylosucrase; transglucosylation; oligosaccharide synthesis; sucrose; erlose; panose

Introduction

Amylosucrase from *Neisseria polysaccharea* (*NpAS*) is an α -transglucosylase of Glycoside-Hydrolase family 13.^{1,2} This sucrose-utilizing enzyme follows a double-displacement mechanism that proceeds via the formation of a covalent β -D-glucosyl enzyme intermediate with a concomitant release of

fructose.³ This intermediate is subsequently attacked either by water molecules (hydrolysis reaction), fructose, glucose or maltooligosaccharides released during the reaction course (Fig. 1). Naturally, the main reaction catalyzed is the formation of soluble maltooligosaccharides and insoluble amylose-like polymer. Transfer onto fructose results in the formation of two sucrose isomers [i.e., turanose (3-O- α -D-glucopyranosyl-D-fructose) and trehalulose (1-O- α -D-glucopyranosyl-D-fructose)]. Three-dimensional structures of *NpAS* in free form (PDB ID:1G5A) or in complex with sucrose (PDB ID: 1JGI) or maltoheptaose (PDB ID: 1MW0) allowed to map the buried catalytic pocket of the enzyme and delineate –1 to +6 subsites.^{4,5} Wild-type *NpAS* catalyzes glucosylation of a large repertoire of exogenous acceptors and naturally reveals a broad promiscuity towards carbo hydrates, polyols or flavonoids.^{6–8} In addition,

Grant sponsor: French National Research Agency (ANR Project GLUCODESIGN); Grant number: ANR-08-PCVI-002-02; Grant sponsor: HPC Resources of the Computing Center of Region Midi-Pyrénées (CALMIP, Toulouse, France).

*Correspondence to: Isabelle André, Laboratoire d'Ingénierie des Systèmes Biologiques et des Procédés, Université de Toulouse, CNRS, INRA, INSA, Toulouse, 31400, France. E-mail: isabelle.andre@insa-toulouse.fr and Magali Remaud-Siméon, Laboratoire d'Ingénierie des Systèmes Biologiques et des Procédés, Université de Toulouse, CNRS, INRA, INSA, Toulouse, 31400, France. E-mail: remaud@insa-toulouse.fr

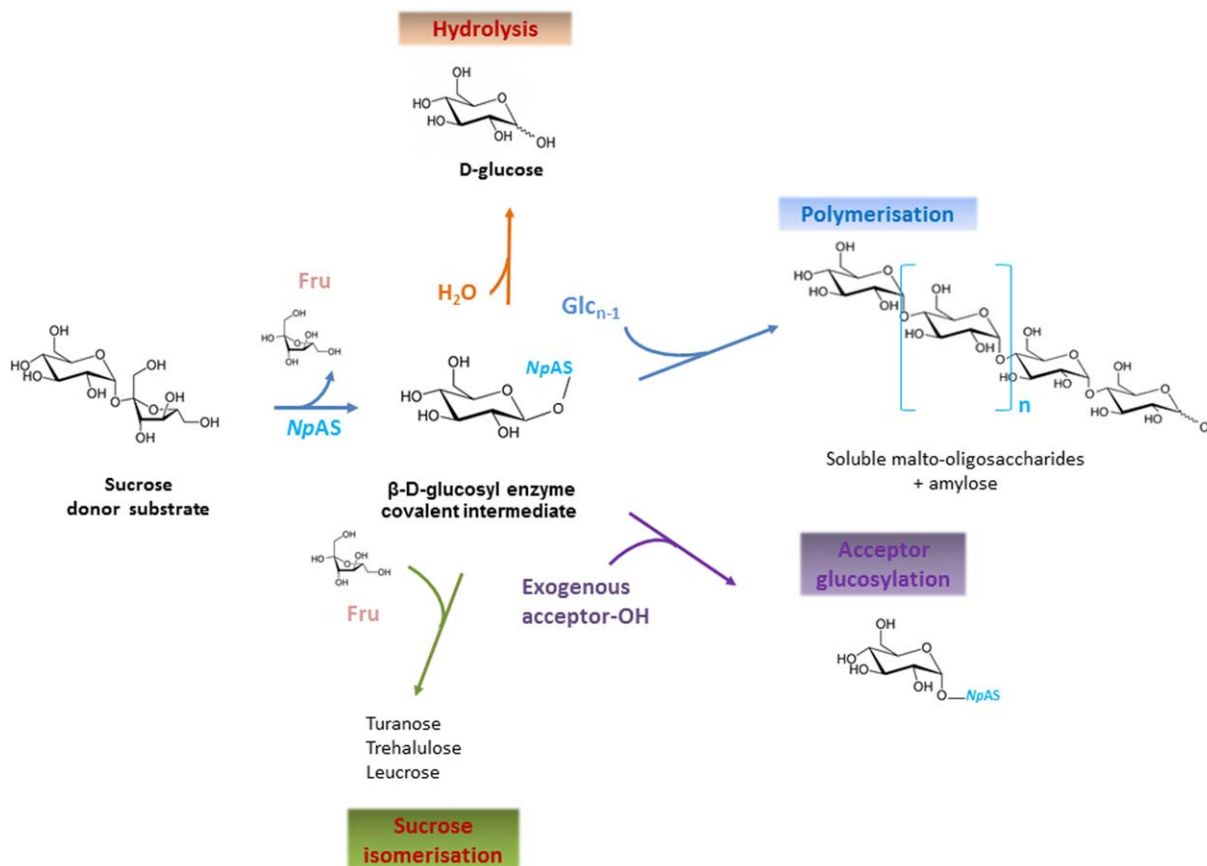


Figure 1. Products synthesized by *NpAS* via the formation of a covalent β-D-glucosyl-enzyme intermediate. The main reaction products are insoluble high molecular weight α-1,4-linked-glucans and soluble malto-oligosaccharides synthesized by polymerization reaction. Glucose is released by hydrolysis. Glucosylation of fructose released during the first reaction step results in the formation turanose, trehalulose, and leucrose by sucrose isomerisation. Glucosylation of exogenous non-natural hydroxylated acceptors can also occur if acceptors are recognized by the enzyme. Fru, fructose; Glc, glucose; Acc, acceptor molecule.

enzyme engineering allowed to evolve *NpAS* and generate mutants with controlled and extended capacity of glucosylation.^{9,10} Site-directed mutagenesis targeting *NpAS* active site enabled the distribution of natural products synthesized from sucrose to be finely tuned.^{11,12} Neutral drift approach and semi-rational design allowed to sort out mutants with drastically improved ability to glucosylate acceptor molecules compared to the parental *NpAS*.^{8,10,13,14}

Very recently, *NpAS* active site was deeply reshaped to adapt the enzyme to the glucosylation of unnatural and slightly protected disaccharides entering in a programmed chemo-enzymatic pathway designed for bacterial antigen synthesis.¹⁵ Using a computer-aided approach, semi-rational libraries, totaling about 2.7×10^4 variants and targeting 23 amino acid positions of subsites +1 and +2 in the active site first shell, were designed. Upon library construction, the mutants were screened, first, on sucrose activity and, next, on their ability to catalyze the glucosylation of the target acceptor, a partially protected β-linked disaccharide, the allyl (2-deoxy-2-trichloroacetamido-β-D-glucopyranosyl)-

(1→2)-α-L-rhamnopyranoside. Whereas only one mutant containing 7 mutations was able to glucosylate the target disaccharide, 55 mutants containing between 5 and 17 mutations were still active on sucrose in spite of their high number of mutations.

The objective of the work disclosed herein was the characterization of this small library of 55 sucrose-active mutants and comparison of parental enzyme and mutant performances to investigate in more details the effect of the mutations introduced at the +1 and +2 subsites of *NpAS* onto the products formed from sucrose substrate. Out of the 55 mutants, 38 showed transglucosylating activities. They were classified on the basis of their product profiles and representative members of each group were deeply studied at both biochemical and structural levels. As a result, several mutants producing trisaccharides, not synthesized by wild-type *NpAS*, and identified as being erlose and panose, were isolated. These biocatalysts could offer alternative routes for the direct production from sucrose of sweeteners or prebiotic molecules.^{16–18}

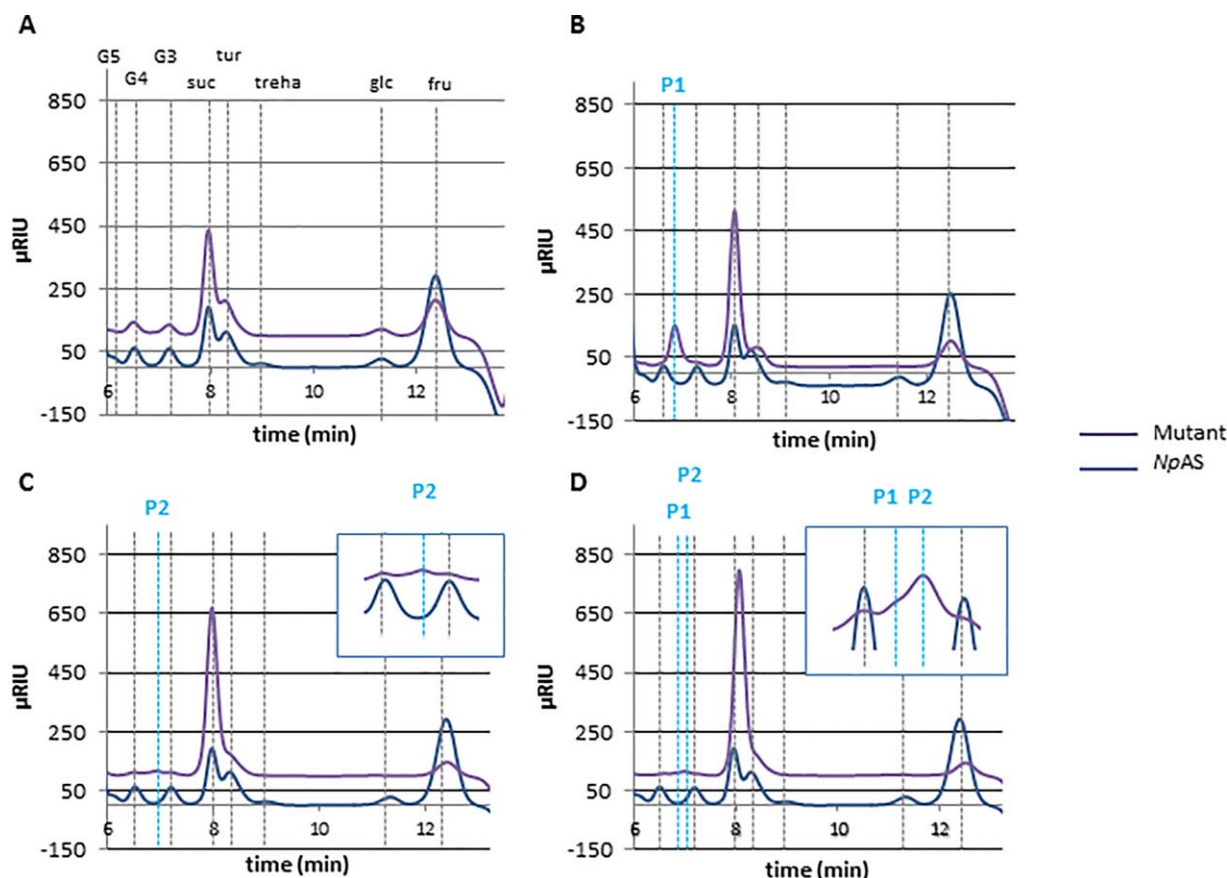


Figure 2. HPLC profiles of products synthesized from 146 mM sucrose after 24 h reactions by wild-type *NpAS* and one representative mutant of each defined group. In purple: product profile for each category of mutants; In blue: profile obtained with wild-type *NpAS*. Profile A corresponds to mutants that synthesize similar products to the wild-type enzyme (Group A). Profile B corresponds to mutants that synthesize a new product P1 (7.2 min), not observed for the wild-type enzyme (Group B). Profile C corresponds to mutants that synthesize novel product P2 (7.0 min), not formed by the wild-type enzyme (Group C). Profile D corresponds to a mutant that synthesizes both P1 and P2 molecules (Group D). Glc, Glucose; Fru, Fructose; Treha, Trehalulose; Tur, Turanose; Suc, Sucrose; G3, maltotriose; G4, maltotetraose; G5, maltopentaose; P1, product 1; P2, product.

Results

Analysis of library screening on sucrose

From semi-rational libraries of *NpAS* mutants designed to tailor novel acceptor specificity toward a partially protected β -linked disaccharide, 55 sucrose-active mutants were isolated.¹⁵ The products synthesized from sucrose with these enzymes were analyzed by HPLC to compare their product profiles and exclude pure sucrose-hydrolases. As a result, 38 variants (out of 55) were identified as being transglucosylases. They contain between 5 and 17 mutations. Despite their high number of mutations, all of them turned out to be more active on sucrose than wild-type *NpAS*. Analysis of their product profiles further showed that 21 mutants synthesize the same products as the wild-type enzyme, although in varying amounts (Fig. 2). On the basis of their HPLC chromatograms, the other mutants were classified in three groups. The first group contains 10 mutants that synthesize, in addition to all natural products, a new product called

P1, not formed by *NpAS*, with a retention time comprised between those of maltotriose and maltotetraose [Fig. 2(B)]. Another group of 6 mutants revealed their ability to produce a second type of molecule P2 (7.2 min) showing a retention time different from that of P1 (7.0 min) and which was not synthesized by parental *NpAS* [Fig. 2(C)]. The last group is composed of only one mutant that is able to synthesize both molecules (P1 and P2) [Fig. 2(D)]. Of note, traces of a product P3 were also found for all three groups.

Characterization and quantification of products synthesized from sucrose

Among mutants able to majorly synthesize P1, P2 or both, the best producer of new compounds (based on peak area comparison at 24 h) was selected as the representative enzyme of each group. This led to the selection of mutant 47A10 for group B, 39A8 for group C and 37G4 for group D. The mutated amino acids in the three selected

Table I. Sequences of the Selected Mutants in Comparison to the Wild-type Enzyme

Amino acid positions		Wild-type	47A10	37G4	39A8
226	Loop 3 (domain B)	R	L	K	K
228		I	V	V	V
229		F	A	F	F
289	Loop 4 (domain A)	A	I	I	I
290		F	Y	Y	Y
300		E	I	I	I
331	Loop 5 (domain A)	V	T	T	T
396	Loop 7 (Domain B')	G	G	S	S
398		T	T	V	V
437		Q	Q	R	S
439		N	N	D	D
445		C	C	C	R
Number of mutations			7	10	11

The 23 targeted positions are shown. In light gray, are highlighted mutated positions compared to wild-type enzyme.

mutants with respect to wild-type *NpAS* are reported in Table I.

All three mutants were then produced, purified to homogeneity and incubated with 146 mM sucrose. Unlike the wild-type *NpAS*, they only produced soluble compounds showing that the polymerization activity was fully abolished for all mutants. The HPAEC-PAD profiles of the soluble products formed are provided in Figure 3. Maltooligosaccharides, turanose and trehalulose are present in all chromatograms. The most striking differences reside in the synthesis of P1 and P2 and the traces of P3 products observed for the mutants while the wild-type *NpAS* was unable to synthesize them. Whereas HPLC chromatograms of our preliminary screening assays indicated only P2 or P1 production for mutants 39A8 and

47A10, respectively, the more sensitive HPAEC-PAD analyses revealed that both P1 and P2 compounds are produced by these mutants. Furthermore, HPAEC-PAD analysis coupled to MS detection indicated a molar mass of m/z 505 g/mol $[ES + H^+]$ for P1, P2 and P3 showing that all compounds are trisaccharides. The reaction mixes were submitted to the action of an invertase and an α -amylglucosidase and digestions were further analyzed by HPAEC-PAD. Product P1 was cleaved by the invertase to yield maltose and fructose while P2 was not (data not shown). Furthermore, amylglucosidase hydrolysis yielded glucose and sucrose from P1 and glucose and maltose from P2. These results suggested that P1 corresponds to erlose, α -D-glucopyranosyl-(1 \rightarrow 4)- α -D-glucopyranosyl-(1 \rightarrow 2)- β -D-Fructose and that P2 corresponds to panose, α -D-glucopyranosyl-(1 \rightarrow 6)- α -D-glucopyranosyl-(1 \rightarrow 4)- α -D-glucose. This was confirmed by the retention times of pure commercial

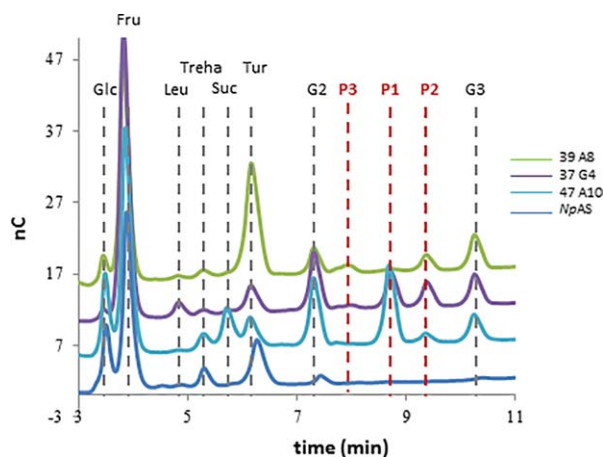


Figure 3. HPAEC-PAD product profiles obtained after 24 h of reaction in the presence of 146 mM sucrose and 1 U mL⁻¹ purified enzyme. The profile of mutant 37G4 is shown in purple, mutant 39A8 in green, mutant 47A10 in cyan and the wild-type *NpAS* is in blue. Glc, Glucose; Fru, Fructose; Treh, Trehalulose; Tur, Turanose; Suc, Sucrose; Leu, Leucrose; G₂, Maltose; P1, product 1; P2, product 2; P3, product; G₃, maltotriose.

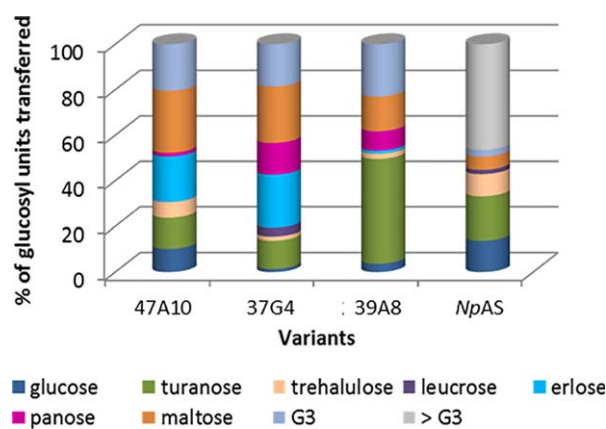


Figure 4. Percentage of glucosyl units transferred from sucrose to the various products with mutants 47A10, 39A8, 37G4 and wild-type *NpAS* after 24 h of reaction. Reactions were performed with 146 mM sucrose and 1 U mL⁻¹ of each enzyme. G: Glucose. The percentages were determined from HPAEC analysis.

Table II. Determination of Apparent Kinetic Parameters and Thermostability Values of Mutants 47A10, 39A8, and 37G4 and Wild-type NpAS

Enzymes	k_{cat} (s^{-1})	K_{m} (mM)	$k_{\text{cat}}/K_{\text{m}}$ ($\text{s}^{-1} \text{mM}^{-1}$)	Behavior	T_{m} ($^{\circ}\text{C}$)
NpAS^a	1.3	50.2	0.026	Saturation	49.0
47A10	n.d.	n.d.	0.015	Linear	46.0
37G4	n.d.	n.d.	0.012	Linear	46.0
39A8	4.5	78.43	0.058	Saturation	47.1

^a Data from Ref. 4, for sucrose > 20 mM.

erlose and panose. Because of the very low level of P3 production, its molecular structure could not be elucidated.

The percentage of glucosyl units incorporated from sucrose, in each type of product is reported in Figure 4. Compared to the wild-type NpAS, and in agreement with their loss of polymerase activity, all three mutants incorporated higher amounts of glucosyl units in maltose (27.3% (mutant 47A10); 24.8% (mutant 37G4); 15.3% (mutant 39A8); versus 5.8% for wild-type NpAS) and in maltotriose (20.5% (mutant 47A10); 18.6% (mutant 37G4), 23% (mutant 39A8); versus 2.9% for wild-type NpAS). Compared to the others, the mutant 39A8 is more specialized in turanose production, incorporating nearly 46% of the glucosyl residues in turanose, versus only 19% for the wild-type NpAS. With mutants 47A10 and 37G4, 20% and 23% glucosyl units were incorporated into erlose, respectively. Much lower values were observed with mutant 39A8 (only 1.4%) and none for the wild-type NpAS. In comparison, panose was mainly produced by mutants 37G4 and 39A8, 13.9% and 8.5% of the glucosyl units incorporated into this trisaccharide, respectively. In comparison, the value goes down to 1.6% with mutant 47A10 and it is not produced by the wild-type NpAS.

Determination of kinetic parameters and stability

The steady-state kinetic parameters (k_{cat} , K_{m} , $k_{\text{cat}}/K_{\text{m}}$) were determined for all purified enzymes upon varying sucrose concentrations from 5 to 600 mM (Table II). Only mutant 39A8 showed a standard saturation kinetic behavior comparable to that observed for the wild-type enzyme and its $k_{\text{cat}}/K_{\text{m}}$ value was found increased by 2.2 fold. Regarding mutants 47A10 and 37G4, no saturation behavior was observed in these conditions suggesting that K_{m} values might be very high. Linear plots correctly fitted initial rate of sucrose consumption versus sucrose concentration. Consequently, catalytic efficiencies were determined from the slope of the linear regression of initial rates of transglucosylation measured according to variable substrate concentrations. The $k_{\text{cat}}/K_{\text{m}}$ values towards sucrose of both mutants decreased by 1.7 fold (47A10) and 2.1 fold (37G4) compared to that of NpAS.

Thermal stability of all three mutants was assessed using circular dichroism. T_{m} values are also listed in Table II. Overall, the high number of buried mutations introduced had a low impact on thermal stability as T_{m} values were found slightly lowered compared to those of wild-type NpAS (-1.9°C for 39A8; -3°C for 47A10 and 37G4, respectively) with regard to (Table I).

Optimization of erlose and panose production

Reactions were performed at various sucrose concentrations (146, 400, and 600 mM). At 400 and 600 mM, sucrose was not fully consumed after 24 h reaction with mutant 47A10, indicating a possible inhibition by the substrate, which was also observed with mutant 37G4 at 600 mM sucrose (Table III). Nevertheless, for all mutants, erlose production was significantly improved at high sucrose concentration, the best values being obtained at 600 mM. As seen in Figure 5, increasing sucrose concentration greatly favored acceptor reaction onto sucrose. As a result, the percentage of glucosyl units incorporated into erlose increased by 2.9 fold (47A10), 2.7 fold (37G4) and 4.6 fold (39A8) at 600 mM in comparison to the values observed at 146 mM sucrose. In these

Table III. Erlose and Panose Production Data Using Mutants of NpAS

	47A10	37G4	39A8
146 mM sucrose = 50 g L⁻¹			
Sucrose consumption, %	87.2	98.7	98.8
Erlose production, g L ⁻¹	6.4	8.5	0.5
Erlose production yield ^a	14.7	17.2	1.0
Panose production, g L ⁻¹	0.4	3.4	2.1
Panose production yield ^b	0.8	6.8	4.2
400 mM sucrose = 137 g L⁻¹			
Sucrose consumption, %	65.5	95.0	96.9
Erlose production, g L ⁻¹	36.8	49.4	5.5
Erlose production yield	41.1	38.0	4.1
Panose production, g L ⁻¹	1.5	13.1	1.0
Panose production yield	1.7	10.1	0.8
600 mM sucrose = 205 g L⁻¹			
Sucrose consumption, %	81.2	61.0	94.7
Erlose production, g L ⁻¹	70.6	57.5	9.6
Erlose production yield	42.4	45.9	4.9
Panose production, g L ⁻¹	3.8	8.0	1.5
Panose production yield	2.3	6.4	0.8

^a Erlose production yield = [erlose (g L⁻¹)]/[sucrose consumed (g L⁻¹).

^b Panose production yield = [panose (g L⁻¹)]/[sucrose consumed (g L⁻¹)].

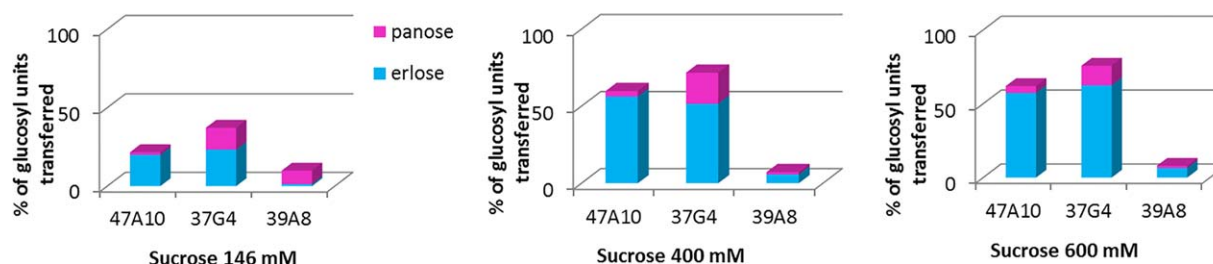


Figure 5. Incorporation of glucosyl units from sucrose into erlose (in cyan) and panose (in magenta) at 146, 400, and 600 mM sucrose with mutants 47A10, 37G4, and 39A8.

conditions, concentrations of erlose attained 70.6, 57.5, and 9.6 g L⁻¹ with corresponding yields of 42, 46, and 5% in the reactions catalyzed by mutants

47A10, 37G4, and 39A8, respectively. In contrast, increasing sucrose concentration had a limited impact on panose yield (Fig. 5).

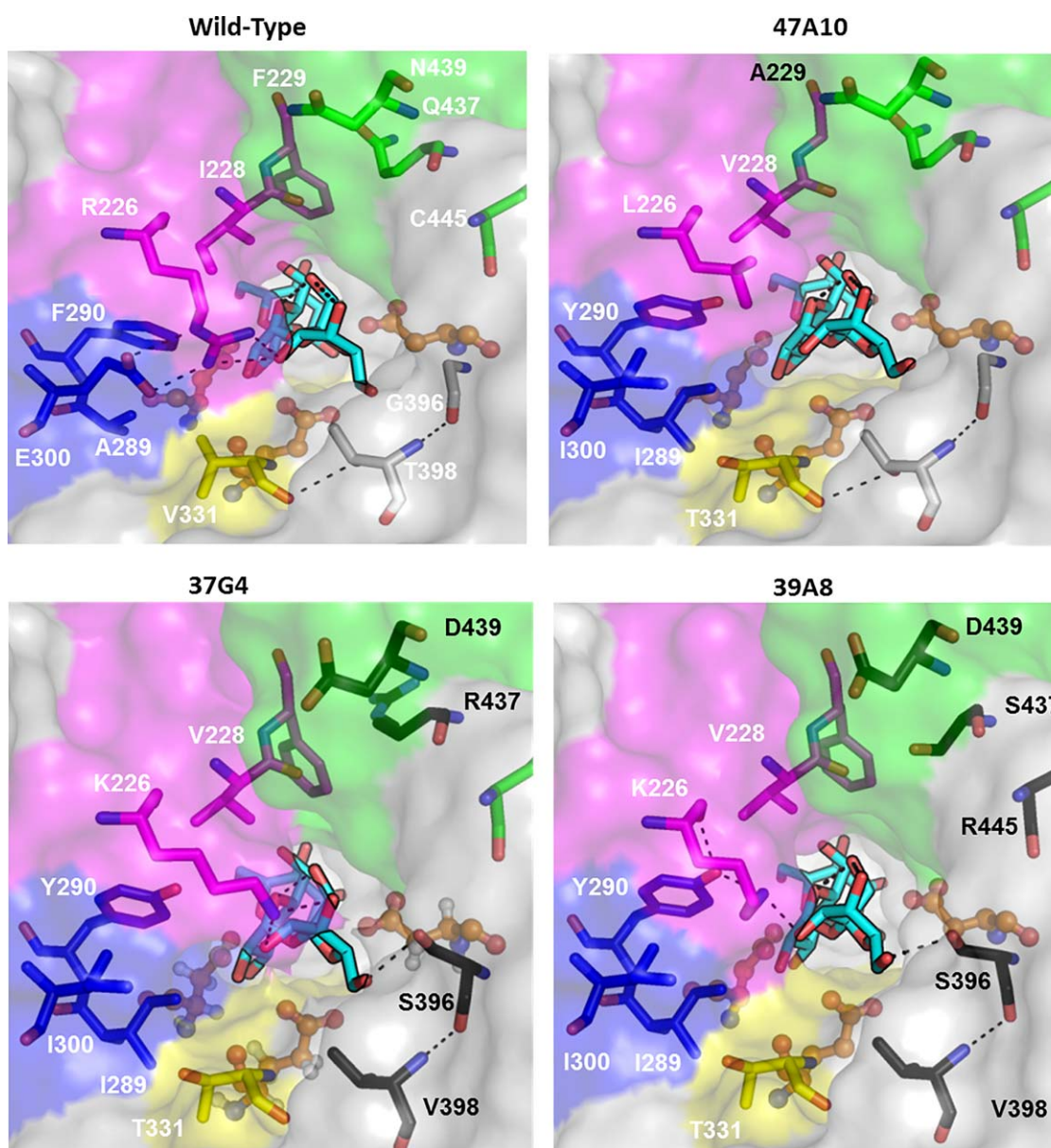


Figure 6. Molecular docking of erlose in wild-type *NpAS* and its mutants 47A10, 37G4, and 39A8. Mutated positions are shown and coloured depending on the loop they belong to. Loops 3, 4, 5, and 7 are colored in magenta, blue, yellow and green, respectively. Labelled in white are highlighted commonly mutated positions and in black are shown mutated positions that are specific to the mutants. Catalytic residues are shown in ball and stick.

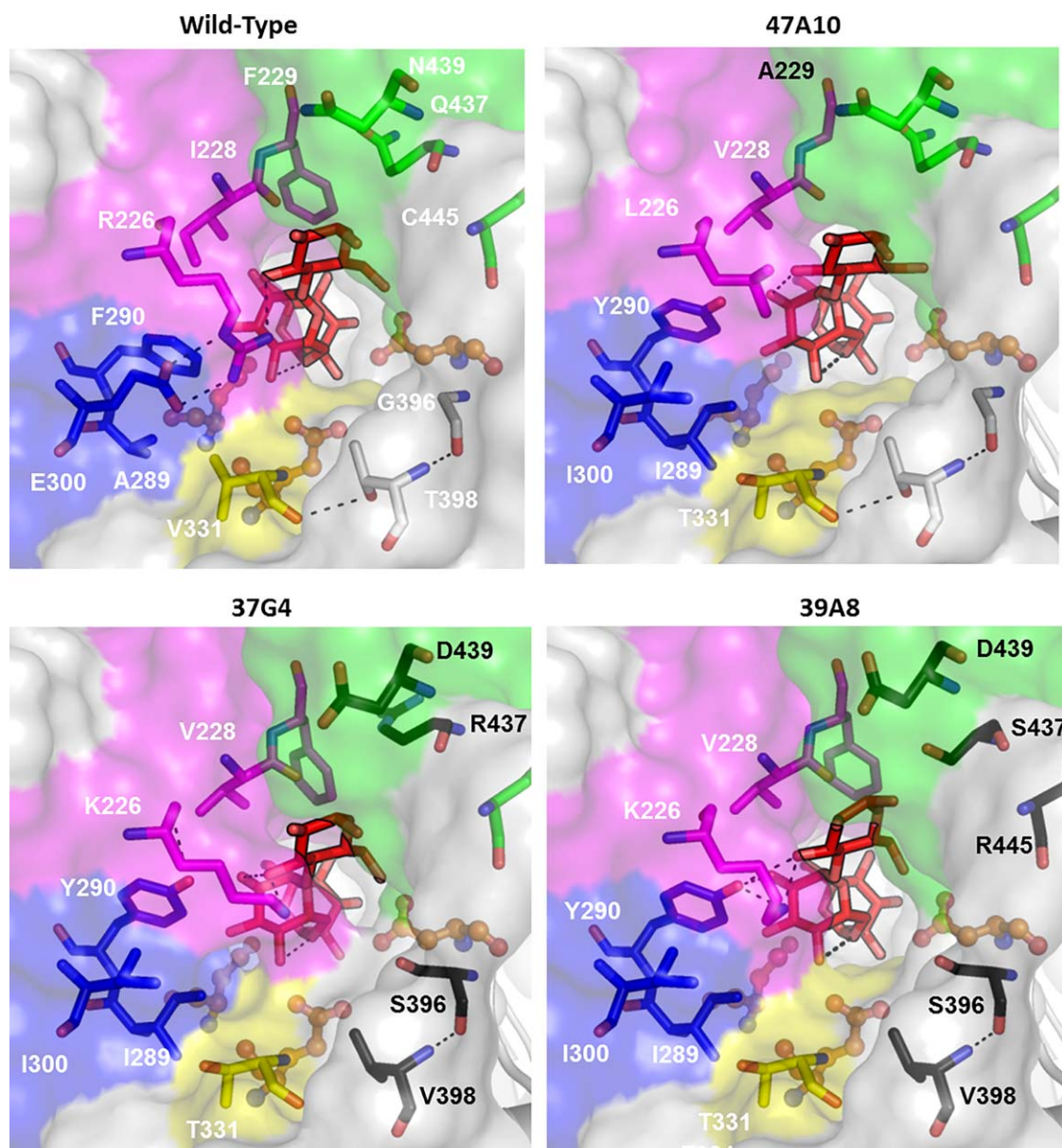


Figure 7. Molecular docking of panose in wild-type *NpAS* and its mutants 47A10, 37G4, and 39A8. Mutated positions are shown and coloured depending on the loop they belong to. Loops 3, 4, 5, and 7 are colored in magenta, blue, yellow and green, respectively. Labelled in white are highlighted commonly mutated positions and in black are shown mutated positions that are specific to the mutants. Catalytic residues are shown in ball and stick.

Structural insight on the effect of mutations onto novel product specificity toward erlose and panose

To investigate further the molecular determinants possibly involved in the product specificity, three-dimensional models of the enzymes in complex with the various products of interest (maltotriose, turanose, erlose, panose) were built and analyzed in details (Figs. 6 and 7). Six amino acid positions (226, 228, 289, 290, 300, and 331) are found commonly mutated in the three variants (Table I). Among them, only position 226 differs in the type of mutation as the arginine is found respectively mutated by a lysine in mutants 37G4 and 39A8 and by a

leucine in mutant 47A10. These six positions belong respectively to loop 3 (residues 224–236), loop 4 (residues 285–303) and loop 5 (residues 327–332) of the catalytic barrel (Figs. 6 and 7). They have been shown to be highly flexible by molecular dynamics simulations¹⁴ and assumed to play a determinant role in the formation of the active site topology and catalytic mechanism of the enzyme.^{19–21} In particular, Arg226 residue in native *NpAS* has been reported to be engaged in a salt bridge with Glu300, controlling the shape of +2/+3 subsites and hampering binding of long acceptors. Mutation of residues 226 and 300 leads thus to a disruption of the salt bridge and a reorganization of the interactions at

+1 and +2 subsites with mutated residues V331T, I228V, A289I and F290Y. In particular, mutation of Arg226 was found to open up the active site around +3 subsite, likely interfering with the binding of oligosaccharides longer than DP3.¹² In mutant 47A10, only one additional mutation, F229A, was found in addition to the six commonly mutated positions. Docking of erlose molecule, the main product formed by this mutant, suggested that fructofuranosyl moiety is stabilized at +2 subsite by hydrogen bonding interactions of fructose (O₃H) with R446 side chain and I330 carbonyl group (Fig. 6). In comparison with maltotriose binding mode, docking of panose in mutants 39A8 and 37G4 indicates a shift of glucopyranosyl units at +1 and +2 subsites due to the α -1,6 linkage present in the molecule (Fig. 7). As a result, all hydrogen bonding network stabilizing the glucopyranosyl moieties at +1 and +2 subsites is altered. Mutations G396S, T398V and N439D are present in both mutants 39A8 and 37G4. In particular, mutations G396S and T398V appear to sterically hinder binding at +2/+3 subsites of oligosaccharides longer than DP3. Mutants 39A8 and 37G4 only differ by the amino acid type present at positions 437 and 445. Interestingly, all these mutations are in the vicinity of the +2 subsite and carried by the B' domain (residues 396–460) which is also highly flexible and assumed to be involved in product specificity. Although molecular determinants responsible for the distinct product profiles observed for the two mutants are still unclear, mutant 39A8 was found to produce majorly turanose and 37G4 synthesized mainly both erlose and panose.

Discussion

Semi-rational design is widely viewed as a very efficient approach for tailoring substrate or product specificity of enzymes. Applied to *NpAS* enzyme, a computer aided-approach to engineer subsites +1 and +2 allowed to isolate one mutant still able to produce soluble maltooligosaccharides, although shorter than for the wild-type *NpAS*, from sole sucrose and which also gained a totally new ability to recognize an unnatural and chemically protected disaccharide of interest for novel vaccine elaboration.¹⁵ The redesign of the catalytic pocket led to the isolation of 55 sucrose-active clones out of 63,000 screened clones. In the present work, we examine in more details the properties of these variants in terms of product specificity, efficiency and stability. Indeed, we anticipated that reshaping of subsites +1 and +2 might have impacted these properties in comparison to wild-type *NpAS*. Mutant discrimination, based on product profile, revealed that 62% of active enzymes differed from wild-type *NpAS* and showed a novel product specificity, highlighted by the production of erlose (α -D-glucopyranosyl-(1 \rightarrow 4)- α -D-glucopyranosyl (1 \rightarrow 2)- β -D-Fructose) and panose

(α -D-glucopyranosyl-(1 \rightarrow 6)- α -D-glucopyranosyl-(1 \rightarrow 4)- α -D-glucose) from sucrose substrate. Noteworthy, these mutants were specialized in short oligosaccharide production and lost their ability to transfer glucosyl units onto oligosaccharides of DP higher than 3. The high percentage of hits showing a new product specificity further demonstrates how powerful computer-aided design can be to address the challenge of changing substrate specificity of enzymes. In addition, molecular modelling of the mutants revealed that compared to the wild-type enzyme, abolition of polymerase activity could be assigned to subsites +1 and +2 reshaping by suppression of salt bridge interaction between Arg226 and Glu300 present in wild-type enzyme and mutation of residues G396 and T398 into bulkier residues (substitution by serine or valine residues, respectively) that hamper binding of oligosaccharides longer than DP3 and thus favoring the accumulation of lower size products. Sucrose and natural acceptor binding in mutants 47A10 and 37G4 has also probably been impacted as revealed by the decrease of mutant catalytic efficiency (by two fold) compared to the wild-type enzyme. Noteworthy, with regard to the number of mutations found in the active site, such a decrease remains acceptable. In contrast mutant 39A8 was found more efficient on sucrose substrate than *NpAS*. Increase of catalytic efficiency relative to wild-type *NpAS* is mainly due to a k_{cat} increase. As the mutant produces high amounts of turanose (121 g L⁻¹ with 59% yield at 600 mM sucrose and 23 g L⁻¹ with 46.9% yield at 146 mM) in comparison with wild-type *NpAS*, we can suggest that fructose is much better accommodated by the mutant to react with the covalent β -glucosyl-enzyme intermediate. Interestingly, the introduction of 7–11 mutations in subsites +1 and +2 of *NpAS* mutants allowed the emergence of a new α -1,6 glucosidic linkage specificity revealed by the presence of panose in addition to maltotriose. This indicates a dual accommodation of maltose acceptor at subsite +1, mainly observed for mutant 37G4, which incorporated 13.9 and 18.6% of glucosyl units in panose and maltotriose, respectively. The most striking fact is that all mutants 47A10, 37G4, and 39A8 acquired the ability to use sucrose as acceptor to produce erlose. Both mutants 47A10 and 37G4 efficiently produced erlose, and increasing sucrose concentration favored erlose production over other products, allowing to reach 42 and 46% yields at 600 mM sucrose concentration, respectively. Of the two mutants, mutant 47A10 was the most specific for erlose production. Reshaping of the active site thus promoted sucrose binding at subsites +1 and +2 to the detriment of glucose and maltose in the mutant in comparison with the wild-type *NpAS*. Erlose and panose are interesting bioactive oligosaccharides due to their acariogenic and low-calory value

properties.^{16–18} Erlase is half as sweet as sucrose while providing similar taste.²² Furthermore, it could also be used to prevent crystal formation and browning reaction during heat processed food.^{23,24} Erlase may not be resistant to digestive enzymes and its prebiotic properties remains to be investigated. However, erlose naturally occurs in honey and other natural sources but is naturally present in small amounts. Thus, several enzymatic routes leading to this trisaccharide were previously investigated. One α -glucosidase from *Archachatina ventricosa* of yet unknown GH family was shown to produce erlose from single sucrose.²⁵ A mix of gluco-oligosylfructosides of DP ranging from 3 to 6 was synthesized in which erlose was identified but not quantified. Cyclodextrin glucanotransferase from *thermoanaerobacter* sp. was also shown to produce erlose from cyclodextrin donor and sucrose acceptor. From 16 mM cyclodextrin and 155 mM sucrose, 35 mM erlose was synthesized, which represents 17.6 g L⁻¹.²⁶ Transfructosylation reaction also allowed to produce erlose. However, in all cases, maltose acceptor was required in addition to sucrose donor. Production levels around 138, 163, or 61 g L⁻¹ were obtained with levansucrase from *B. amy-loliquefaciens* (using 0.8 M sucrose/0.4 M maltose,²⁷ *Bacillus subtilis* (0.7 M sucrose/0.7 M maltose²⁸ or inulosucrase from *Lactobacillus gasseri*²⁹ (0.6 M Sucrose/1.17 M Maltose, respectively). Our process of production compares favorably with these alternative enzymatic processes as the mutants of amylosucrase produce erlose in fairly high amounts from sole sucrose. In addition, one of the mutants reported here was also a substantial producer of panose, a trisaccharide of interest also for food industry. It displays similar sweetening properties as erlose, but it also displays anti-fading and antioxidant properties of interest for food industry.³⁰ Several studies have proven its non-digestibility in the upper gastrointestinal tract by *in vitro* assays.^{17,31–35} Numerous synthetic routes to panose exist and the molecule can be produced in high yield via enzymatic processes including hydrolysis of pullulan or starch with pullulanase or α -amylase^{36–39} or by transglucosylation reaction with dextran-sucrase from *L. mesenteroides* from sucrose donor and maltose acceptor^{40–43} and by glycoside-hydrolases from the marine anaspidean mollusk *Aplysia fasciata*.⁴⁴ However, no study reported the direct production of panose from sucrose alone.

In conclusion, this is the first report of novel products obtained from sole sucrose using engineered amylosucrases. Indeed, erlose and panose trisaccharides are not produced by any of the wild-type amylosucrases characterized to date. Yields reported here after optimization of substrate concentrations are quite encouraging as they can surely be further optimized in batch or fed-batch reactors to propose

novel synthetic routes, especially for the production of erlose, directly from an agroresource, sucrose.

Theoretical and Experimental Procedures

Bacterial strains, plasmids, and chemicals

Plasmid pGST-amylosucrase (pGST-AS) derived from the pGEX-6P-3 (GE Healthcare Biosciences, Piscataway, U.S.A) encoding GST fused to *N. polysaccharea* amylosucrase, was used for the construction of semi-rational libraries. *E.coli* TOP 10 electrocompetent cells (Invitrogen, Carlsbad, U.S.A.) were utilized as gene expression and production of recombinant amylosucrase variants. *DpnI*, *EcoRI* HF and *NotI* HF restriction enzymes, T4 DNA ligase and Antarctic Phosphatase were purchased from New England Biolabs (Beverly, MA, U.S.A.). Phusion DNA-polymerase was purchased from Finnzymes (Espoo, Finland). Ampicillin, lysozyme and isopropyl- β -D-thiogalactopyranoside (IPTG) were purchased from Eurodemex (Souffelweyersheim, France); Bromothymol blue was ordered from Sigma-Aldrich (St Louis, MO). Oligonucleotides were synthesized by Eurogentec (Liege, Belgium). DNA plasmid extraction (GenElute HP plasmid Miniprep kit, Qiagen, Chatsworth, CA), DNA purification and gel extraction (GenElute Gel Extraction kit) columns were purchased from Sigma-Aldrich (St Louis, MO). DNA sequencing was performed by GATC Biotech AG (Constance, Germany). Erlase and panose standards were purchased from Carbosynth (Compton, Berkshire, U.K.).

Library construction

The construction of the libraries from which were isolated the mutants characterized herein were previously described.¹⁵ Briefly, the libraries of *NpAS* were initially designed to recognize and glucosylate a partially protected β -linked disaccharide acceptor called allyl 2-deoxy-2-*N*-trichloroacetyl- β -D-glucopyranosyl-(1 \rightarrow 2)- α -L-rhamnopyranoside. Altogether, 63,000 variants were screened using a pH-based assay on solid medium as described earlier.¹⁵ The 55 active clones were stored in 96-well microplates containing LB medium (200 μ L), ampicillin (100 μ g mL⁻¹) and glycerol (12% w/v).

Library screening in microplate format

The 55 mutants were grown at 30°C for 24 h in microtiter plates that serve to inoculate 96-Deep Well plates containing autoinducing media ZYM-5052⁴⁵ supplemented with ampicillin (100 μ g mL⁻¹). After 24 h growth at 30°C, cell lysis was performed by addition of lysozyme (0.5 mg mL⁻¹) and DNase and freezing at -80°C overnight. After thawing at room temperature, microplates were centrifuged (20 min, 3000g, 4°C) to harvest the enzyme extract. The enzyme extract was divided in two fractions. On one

side, 50 μL of the soluble fractions were incubated with 50 μL of 292 mM sucrose solution for 1 h at 30°C. Reactions were stopped by addition of 100 μL of a dinitrosalicylic acid (DNS) solution, heated at 95°C during 10 min. Reaction mixes are then diluted twice or 5-times (for the highest activities) before optical density measurements at 540 nm. The content of reducing sugars was determined from a calibration curve established with fructose standards. 55 clones were confirmed and sequenced on the entire gene by GATC Biotech GA (Constance, Germany). The second part of the enzyme extract (100 μL) was also incubated with sucrose (100 μL at 292 mM) for 24 h at 30°C. The reaction was stopped by heating at 95°C for 5 min. The mix was centrifuged and the supernatant was analyzed by HPLC using an Aminex HP87K column (300 \times 7.8 mm, Biorad) with ultra-pure water at 0.6 mL min⁻¹ as eluent at 65°C. The detection was performed with a Shodex RI 101 series refractometer. The mutants differing from the wild type *NpAS* on the basis of their product profiles were then classified into three groups according to their product profiles. One representative of each group (the best one for production of P1 or P2 or P1/P2 according to peak area at t24 h by RI detection in HPLC) was selected *ie* mutants 47A10, 39A8, 37G4 and produced at higher scale to allow enzyme purification and characterization.

Characterization of the selected mutants

Production and purification. A preculture (50 mL of LB inoculated with 50 μL of stock culture of the selected clones) was performed overnight at 30°C and used to inoculate 1 L of LB + ampicillin at OD600_{nm} = 0.2 and grown at 23°C. Cultures were induced at OD600_{nm} = 0.5 with IPTG and incubated for 17 h. Cells were centrifuged at 5 000 rpm at 4°C for 10 min. The pellet was resuspended in Tris 50 mM, NaCl 150 mM at pH 7 and OD600_{nm} = 80. After sonication, the crude extract was centrifuged at 10 000 Rpm, 20 min, 4°C. Before purification by affinity chromatography on the AKTA Express systems, these supernatants were filtered on a syringe with a Minisart NML filter (Sartorius, Goettingen, Germany) to remove additional cell wastes. Then, they were loaded onto Glutathion Sepharose 4B column (Dutscher, Brumath, France) in the presence of Tris buffer supplemented in EDTA and DTT (50 mM Tris, 150 mM NaCl, 1 mM EDTA, 1 mM DTT, pH 7.0). To maximize protein fixation on gel, the flow through was recycled to be loaded a second time on columns. Then, PreScission protease (Dutscher, Brumath, France) (500 U in 5 mL buffer (50 mM Tris, 150 mM NaCl, 1 mM EDTA, 1 mM DTT, pH 7.0)) was injected and cleavage of GST Tag occurred during 1 night always at 4°C. The next day, protein and

GST Tag were eluted in Deep-Well by fraction of 2 mL in a Deep-Well by UV detection at 280 nm. Protein concentration was estimated using Nano-drop ND-1000 spectrophotometer. Specific activity was determined at 30°C, in 50 mM Tris-HCl buffer pH 7.0, using 50 g L⁻¹ sucrose. Reducing sugar production was determined using dinitrosalicylic acid assay. One unit of amylosucrase activity corresponds to the amount of enzyme that catalyzes the release of 1 μmol of reducing sugars per minute in the assay conditions.

Analysis of product formed from sucrose. Reactions were performed at 30°C during 24 h with 146 mM sucrose in the presence of wild-type enzyme or mutants at 1 U mL⁻¹. Reaction mixes were stopped by heating at 95°C during 5 min. The reaction medium was centrifuged. In contrast to wild-type *NpAS*, the three mutants did not synthesize insoluble products. Supernatants were all diluted at 10 mg L⁻¹ and analyzed by HPAEC using the same column as above coupled to mass spectrometry detection, 1/4 of the flow containing the sample was injected into the MSQ mixed with TFA at 150 mM and formic acid at 0.1% (v/v). Samples were eluted with a gradient of sodium acetate (from 6 to 300 mM in 28 min) in 150 mM NaOH. Detection was performed using a Dionex ED40 module with a gold working electrode and Ag/AgCl reference electrode.

Optimization of erlose and panose production.

Reactions were performed with 1 U mL⁻¹ of each purified mutants or wild-type enzyme in the presence of 146, 400, and 600 mM sucrose concentrations at 30°C during 24 h. Following 5 min heating at 95°C, reaction mixes were centrifuged. The soluble fractions were analyzed by HPAEC-PAD as described above.

Kinetic parameters determination. Initial velocity of sucrose consumption determined from reactions was carried out with pure enzymes (0.07 or 0.1 U mL⁻¹) at sucrose concentrations ranging from 5 to 600 mM and 30°C under agitation. After heating at 95°C and centrifugation, aliquots were analyzed by HPLC RI with a Biorad HPX-87K column to determine sucrose consumed and fructose release. Eight samples were taken at regular time intervals that were determined in order to ensure that <5% of the sucrose substrate was consumed before the end of the kinetic experiments. Fructose release was monitored by HPLC-RI with a Biorad HPX-87K column.

Stability studies. The melting point (T_m) of amylosucrase mutants was determined by Circular Dichroism analysis on a JASCO J815 spectropolarimeter, using a Peltier cell temperature controller

with a thermal transition monitored from 20 to 80°C. Purified enzymes were diluted at 2 μ M in Tris buffer (50 mM Tris, 150 mM NaCl, 1 mM DTT, 1 mM EDTA, pH 7.0).

Computational Procedures

Starting coordinates were extracted from the crystallographic structure of *NpAS* in complex with sucrose (PDB ID: 1JGI)⁴⁶ to generate 3D models of the different enzymes of interest and mutations were introduced using the Biopolymer module of the InsightII software package (Accelrys). The conformations of the mutated residue side chains were optimized by manually selecting a low-energy conformation from a side-chain rotamer library. Steric clashes (van der Waals overlap) and non-bonded interaction energies (Coulombic and Lennard-Jones) were evaluated for the various side-chain conformations. The 3D models were then refined using the CFF91 force field implemented within the DISCOVER module of InsightII software suite (Accelrys, San Diego, CA). For the minimization, the CFF91cross terms, a harmonic bond potential, and a dielectric of 1.0 were used. An initial minimization with a restraint on the protein backbone was performed using a steepest descent algorithm followed by conjugated gradient minimization steps until the maximum RMS was <0.1. In a subsequent step, the system was fully relaxed. Using as templates the three dimensional structures of *NpAS* co-crystallized with sucrose (PDB ID: 1JGI),⁴⁶ maltoheptaose (PDB ID: 1MW0)⁴⁷ and turanose (PDB ID: 3UEQ),⁴⁸ we have built models for the wild-type *NpAS* and the three selected mutants in complex with molecules of interest, maltotriose, panose, erlose and turanose. Models were then subjected to the same energy minimization procedure described above from sucrose. Graphics were done using Pymol (Schrodinger, Portland, OR).

Acknowledgments

The authors are grateful to G. Cioci and S. Tranier in using the PICT facility for protein biophysical characterization, N. Monties for her help in the product analysis by HPAEC-PAD and HPAEC-PAD-MS of the ICEO high-throughput facility, devoted to the engineering and screening of new and original enzymes, of the Laboratoire d'Ingénierie des Systèmes Biologiques et des Procédés (Toulouse, France). This work was granted access to the HPC resources of the Computing Center of Region Midi-Pyrenees (CALMIP, Toulouse, France).

References

1. Cantarel BL, Coutinho PM, Rancurel C, Bernard T, Lombard V, Henrissat B (2009) The carbohydrate-

- active enzymes database (CAZy): an expert resource for glycogenomics. *Nucleic Acids Res* 37:D233–D238.
2. Lombard V, Golaconda Ramulu H, Drula E, Coutinho PM, Henrissat B (2014) The carbohydrate-active enzymes database (CAZy) in 2013. *Nucleic Acids Res* 42:D490–D495.
3. McCarter JD, Withers SG (1994) Mechanisms of enzymatic glycoside hydrolysis. *Curr Opin Struct Biol* 4: 885–892.
4. Potocki de Montalk G, Remaud-Siméon M, Willemot RM, Planchot V, Monsan P (1999) Sequence analysis of the gene encoding amylosucrase from *Neisseria polysaccharea* and characterization of the recombinant enzyme. *J Bacteriol* 181:375–381.
5. Potocki de Montalk G, Remaud-Siméon M, Willemot RM, Sarçabal P, Planchot V, Monsan P (2000) Amylosucrase from *Neisseria polysaccharea*: novel catalytic properties. *FEBS Lett* 471:219–223.
6. Daudé D, Champion E, Morel S, Guieysse D, Remaud-Siméon M, André I (2013) Probing substrate promiscuity of amylosucrase from *Neisseria polysaccharea*. *ChemCatChem* 5:2288–2295.
7. André I, Potocki-Veronese G, Morel S, Monsan P, Remaud-Siméon M (2010) Sucrose-utilizing transglucosidases for biocatalysis. *Top Curr Chem* 294:25–48.
8. Malbert Y, Pizzut-Serin S, Massou S, Cambon E, Laguerre S, Monsan P, Lefoulon F, Morel S, André I, Remaud-Siméon M (2014) Extending the structural diversity of α -flavonoid glycosides with engineered glucanases. *ChemCatChem* 6:2282–2291.
9. Van der Veen B, Potocki-Véronèse G, Albenne C, Joucla G, Monsan P, Remaud-Siméon M (2004) Combinatorial engineering to enhance amylosucrase performance: construction, selection, and screening of variant libraries for increased activity. *FEBS Lett* 560:91–97.
10. Champion E, André I, Moulis C, Boutet J, Descroix K, Morel S, Monsan P, Mulard LA, Remaud-Siméon M (2009) Design of alpha-transglucosidases of controlled specificity for programmed chemoenzymatic synthesis of antigenic oligosaccharides. *J Am Chem Soc* 131: 7379–7389.
11. Albenne C, Skov LK, Mirza O, Gajhede M, Potocki-Veronese G, Monsan P, Remaud-Siméon M (2002) Maltooligosaccharide disproportionation reaction: an intrinsic property of amylosucrase from *Neisseria polysaccharea*. *FEBS Lett* 527:67–70.
12. Cambon E, Barbe S, Pizzut-Serin S, Remaud-Siméon M, André I (2014) Essential role of amino acid position 226 in oligosaccharide elongation by amylosucrase from *Neisseria polysaccharea*. *Biotechnol Bioeng* 111: 1719–1728.
13. Daudé D, Remaud-Siméon M, André I (2013) Molecular evolutionary perspectives of amylosucrases: from substrate promiscuity to tailored catalysis. PhD dissertation, INSA de Toulouse. <https://www.theses.fr/2013ISAT0036>
14. Champion E, Guérin F, Moulis C, Barbe S, Tran TH, Morel S, Descroix K, Monsan P, Mourey L, Mulard LA, Tranier S, Remaud-Siméon M, André I (2012) Applying pairwise combinations of amino acid mutations for sorting out highly efficient glucosylation tools for chemo-enzymatic synthesis of bacterial oligosaccharides. *J Am Chem Soc* 134:18677–18688.
15. Vergès A, Cambon E, Barbe S, Salamone S, Le Guen Y, Moulis C, Mulard LA, Remaud-Siméon M, André I (2015) Computer-aided engineering of a transglycosylase for the glucosylation of an unnatural disaccharide of relevance for bacterial antigen synthesis. *ACS Catal* 5:1186–1198.

16. Skov LK, Mirza O, Henriksen A, De Montalk GP, Remaud-Siméon M, Sarçabal P, Willemot RM, Monsan P, Gajhede M (2001) Amylosucrase, a glucan-synthesizing enzyme from the alpha-amylase family. *J Biol Chem* 276:25273–25278.
17. Albenne C, Skov LK, Mirza O, Gajhede M, Feller G, D'Amico S, André G, Potocki-Véronèse G, Van der Veen B, Monsan P, Remaud-Siméon M (2004) Molecular basis of the amylose-like polymer formation catalyzed by *Neisseria polysaccharea* amylosucrase. *J Biol Chem* 279:726–734.
18. Skov LK, Mirza O, Henriksen A, De Montalk GP, Remaud-Siméon M, Sarçabal P, Willemot RM, Monsan P, Gajhede M (2000) Crystallization and preliminary X-ray studies of recombinant amylosucrase from *Neisseria polysaccharea*. *Acta Cryst D* 56:203–205.
19. Yamasaki Y, Suzuki Y (1980) α -Glucosidase and glucoamylase from molds. *J Jpn Soc Starch* 27:74–83.
20. Kohmoto T, Fukui F, Takaku H, Machida Y, Arai M, Mitsuoka T (1988) Effect of isomalto-oligosaccharides on human fecal flora. *Bifidobact Microflora* 7:61–69.
21. Miyake T, Yoshida M, Takeuchi K (1985). Imparting low- or anti-cariogenic property to orally usable products, Patent, US 4518581 A.
22. Côté GL (2007) Novel enzyme technology for food applications. Elsevier, pp 243–269. <http://pubs.rsc.org/-/content/articlelanding/1955/jr/jr9550000355#divAbstract>.
23. Prapulla SG, Subhaprada V, Karanth NG (2000) Microbial production of oligosaccharides: a review. *Adv Appl Microbiol* 47:299–343.
24. Yamada T, Kimura S, Igarashi K (1980) Metabolism of glucosylsucrose and maltosylsucrose by *Streptococcus mutans*. *Caries Res* 14:139–147.
25. Soro RY, Diopoh JK, Willemot RM, Combes D (2007) Enzymatic synthesis of polyglucosylfructosides from sucrose alone by a novel α -glucosidase isolated from the digestive juice of *Archachatina ventricosa* (Achatinidae). *Enzyme Microb Technol* 42:44–51.
26. Tian F, Karboune S (2012) Enzymatic synthesis of fructooligosaccharides by levansucrase from *Bacillus amyloliquefaciens*: specificity, kinetics, and product characterization. *J Mol Catal B Enzym* 82:71–79.
27. Canedo M, Jimenez-Estrada M, Cassani J, Lopez-Munguia A (1999) Production of maltosylfructose (erlose) with levansucrase from *Bacillus subtilis*. *Biocat Bio-transform* 16:475–485.
28. Díez-Municio M, de las Rivas B, Jimeno ML, Muñoz R, Moreno FJ, Herrero M (2013) Enzymatic synthesis and characterization of fructooligosaccharides and novel maltosylfructosides by inulosucrase from *Lactobacillus gasseri* DSM 20604. *Appl Environ Microbiol* 79:4129–4140.
29. Higashimura Y, Emura K, Kuze N, Shirai J, Koda T (2001) Fading Inhibitors, Patent, CA 2378464 A1.
30. Chung CH, Day DF (2002) Glucooligosaccharides from *Leuconostoc mesenteroides* B-742 (ATCC 13146): a potential prebiotic. *J Ind Microbiol Biotechnol* 29:196–199.
31. Chung CH, Day DF (2004) Efficacy of *Leuconostoc mesenteroides* (ATCC 13146) isomaltoligosaccharides as a poultry prebiotic. *Poult Sci* 83:1302–1306.
32. Machida Y, Fukui F, Komoyo T (1986) Promoting the proliferation of intestinal bifidobacteria, Patent, US 4782045 A.
33. Mäkeläinen H, Hasselwander O, Rautonen N, Ouwehand AC (2009) Panose, a new prebiotic candidate. *Lett Appl Microbiol* 49:666–672.
34. Charalampopoulos D, Rastall RA (2012) Prebiotics in foods. *Curr Opin Biotechnol* 23:187–191.
35. Thompson A, Wolfrom ML (1951) Degradation of amylopectin to panose. *J Am Chem Soc* 73:5849–5850.
36. Sakano Y, Kogure M, Kobayashi T, Tamura M, Suekane M (1978) Enzymatic preparation of panose and isopanose from pullulan. *Carbohydr Res* 61:175–179.
37. Gibson GR, Probert HM, Loo JV, Rastall RA, Roberfroid MB (2004) Dietary modulation of the human colonic microbiota: updating the concept of prebiotics. *Nutr Res Rev* 17:259–275.
38. Stanley P, Whelan WJ, Edwards TE (1955) Polysaccharides of Baker's yeast. Part I. Glycogen. *J Chem Soc* 355–359. <http://pubs.rsc.org/-/content/articlelanding/1955/jr/jr9550000355#divAbstract>.
39. Suzuki J (1988) Enzymatic synthesis of glycosides. *J Jpn Soc Starch Sci* 35:93–102.
40. Kitahata S (1990) Synthesis of oligosaccharides using microbial enzymes. *J Jpn Soc Starch Sci* 37:49–67.
41. Robyt JF, Eklund SH (1983) Relative, quantitative effects of acceptors in the reaction of *Leuconostoc mesenteroides* B-512F dextranase. *Carbohydr Res* 121:279–826.
42. Robyt JF, Walseth TF (1978) The mechanism of acceptor reactions of *Leuconostoc mesenteroides* B-512F dextranase. *Carbohydr Res* 61:433–445.
43. Andreotti G, Giordano A, Tramice A, Mollo E, Trincione A (2006) Hydrolyses and transglycosylations performed by purified alpha-d-glucosidase of the marine mollusc *Aplysia fasciata*. *J Biotechnol* 122:274–284.
44. Studier FW (2005) Protein production by auto-induction in high density shaking cultures. *Protein Expr Purif* 41:207–234.
45. Mirza O, Skov LK, Remaud-Siméon M, Potocki De Montalk G, Albenne C, Monsan P, Gajhede M (2001) Crystal structures of amylosucrase from *Neisseria polysaccharea* in complex with D-glucose and the active site mutant Glu328Gln in complex with the natural substrate sucrose. *Biochemistry* 40:9032–9039.
46. Skov LK, Mirza O, Sprogø D, Dar I, Remaud-Siméon M, Albenne C, Monsan P, Gajhede M (2002) Oligosaccharide and sucrose complexes of amylosucrase. Structural implications for the polymerase activity. *J Biol Chem* 277:47741–47747.
47. Guérin F, Barbe S, Pizzut-Serin S, Potocki-Véronèse G, Guieysse D, Guillet V, Monsan P, Mourey L, Remaud-Siméon M, André I, Tranier S (2012) Structural investigation of the thermostability and product specificity of amylosucrase from the bacterium *Deinococcus geothermalis*. *J Biol Chem* 287:6642–6654.
48. Monthieu C, Guibert A, Taravel FR, Nardin R, Combes D (2003) Purification and characterization of polyglucosylfructosides produced by means of cyclodextrin glucosyltransferase. *Biocat Biotrans* 21:7–15.